J. Phys. B: At. Mol. Opt. Phys. **23** (1990) 2117-2130. Printed in the UK

Cross sections for K-shell ionisation by electron impact†

Ricardo Mayol and Francesc Salvat

Facultat de Física (ECM), Universitat de Barcelona and Societat Catalana de Física (IEC), Diagonal 647, E-08028 Barcelona, Spain

Received 29 December 1989

Abstract. A semi-phenomenological method to compute the cross section for bound shell ionisation of atoms by impact of relativistic electrons is proposed. This method involves a simple schematisation of the Bethe surface, which is obtained from the experimental optical oscillator strength distribution. Our approach may be used to describe the ionisation from any bound shell. We consider in detail the case of K-shell ionisation and derive an analytical formula for the differential cross section on the basis of a hydrogenic optical oscillator strength density. Close collisions are described by the Moller differential cross section, thus incorporating exchange effects. Empirical corrections to the Born approximation for energies near the ionisation threshold are introduced. The relationship of our approximation and the Weizsacker-Williams method of virtual quanta is also discussed.

1. Introduction

Cross section data for inner-shell ionisation by electron impact are required for quantitative elemental analysis in three different techniques for material characterisation: electron-probe microanalysis, Auger electron spectroscopy and electron energy-loss spectroscopy. Cross sections for production of ionised states are also needed in the description of the interactions of radiation with matter as well as for a quantitative understanding of radiation damage.

Powell (1985) gives a comprehensive review of experimental data, theoretical calculations and semi-empirical formulae for inner-shell ionisation. Such empirical formulae are very useful in algorithms for elemental quantitative analysis even though they have been derived from a limited base of experimental and calculated cross sections and there is a risk of using them beyond the range of conditions for which they were developed. On the other hand, experimental and theoretical information on the energy-loss differential cross section (DCS) is scarce although this is the key quantity for a detailed description of the production of ionised states which could be obtained, for instance, through Monte Carlo simulation.

Recently Ashley (1982, 1988) and Penn (1987) have proposed semi-empirical methods to describe the inelastic interactions of low energy electrons with condensed matter in terms of the optical properties of the considered medium. These methods are reminiscent of the statistical model of Lindhard and Scharff (1953)—see also Tung *et al* (1979)—where the stopping medium is viewed as an inhomogeneous electron gas and the differential inverse mean free path (DIMFP) is obtained as an average of the DIMFPS in free electron gases of different densities. The essential difference between

† Supported in part by the Comisión Interministerial de Ciencia y Tecnología (Spain), contract no PB86-0589.

0953-4075/90/122117+14$03.50

the statistical model and the approaches of Ashley and Penn lies in the weights used to average the free electron gas DIMFPS. The average in the statistical model is performed according to the local electron density of the medium, whereas the latter methods use experimental optical dielectric data. In the following, these kinds of semi-empirical approaches will be referred to as statistical models.

We give here a survey of the statistical models from an atomistic point of view. These models contain two basic ingredients: the optical oscillator strength (OOS) distribution and the generalised oscillator strength (GOS) per electron. The various approaches proposed to date differ in the adopted OOS and GOS per electron and are limited to non-relativistic energies.

In the present paper we describe a new statistical model and we use it to compute K-shell ionisation cross sections. This model incorporates a simple GOS per electron, which facilitates the introduction of relativistic effects as well as exchange and low energy corrections to the Born approximation. The OOS for K-shell ionisation or, equivalently, the photoelectric cross section are approximated from the modified hydrogenic model (Egerton 1986) which leads to an explicit analytical expression for the differential cross section (DCS). The evaluation of the DCS for other shells may be performed in a similar way, but then one needs to develop a satisfactory algorithm for determining the component of the (experimental) OOS associated with ionisation of the considered shell. The model yields K-shell ionisation cross sections in good agreement with experimental data up to highly relativistic energies. Our results also agree with the *ab initio* calculations of Scofield (1978).

The Weizsacker-Williams method of virtual quanta (Jackson 1975) is known to yield fairly accurate cross sections for inner shell ionisation (Kolbensvedt 1967, Seltzer and Berger 1982), at least for kinetic energies well above the ionisation threshold. Actually, the method of virtual quanta and the statistical models are built on the same physical assumption, i.e. that the response of the target is mainly determined by its optical properties. A closer relationship between the method of virtual quanta and the statistical models emerges in a natural way when relativistic effects are introduced in the latter. In particular, we will show that the Weizsacker-Williams method, as used by Kolbensvedt (1967), leads to exactly the same inelastic cross sections as a statistical model with a suitable GOS per electron.

In section 2 we give a summary of basic formulae concerning the relativistic Born approximation. After a brief description of the non-relativistic statistical models, we present our relativistic model in section 3 where we also give the modified hydrogenic OOS that we have adopted to describe K-shell ionisations. Low energy corrections and exchange effects are introduced in section 4 by following semi-empirical arguments. The relationship of the present statistical model and the method of virtual quanta is discussed in section 5. Section 6 is devoted to the comparison of K-shell ionisation cross sections, obtained from the statistical model and from the Weizsacker-Williams method, with experimental data.

2. The generalised oscillator strength

Inelastic collisions of electrons with kinetic energy E, with a target atom of atomic number Z are conveniently described in terms of the energy loss W and the recoil energy Q. This last quantity is defined by (Fano 1963)

$$Q(1+Q/2mc^2)=q^2/2m \qquad \text{or} \qquad Q=[(cq)^2+m^2c^4]^{1/2}-mc^2 \tag{1}$$

where $\boldsymbol{q}$ is the momentum transfer. The Born DCS for energy loss W and recoil energy Q is given by (Fano 1963, Fano and Cooper 1968, Mayol and Salvat 1989)

$$\frac{d^2\sigma}{dQ\,dW}=\frac{2\pi e^4}{mv^2}\left[\frac{1}{WQ(1+Q/2mc^2)}+\frac{\beta_t^2 W/2mc^2}{\{Q(1+Q/2mc^2)-W^2/2mc^2\}^2}\right]\frac{df(Q,W)}{dW} \tag{2}$$

where $df(Q, W)/dW$ is the generalised oscillator strength (GOS) per unit energy loss, m and e are the electron mass and charge, v is the velocity of the incident electron and β_t is the component of $\boldsymbol{\beta}\equiv\boldsymbol{v}/c$ perpendicular to the momentum transfer $\boldsymbol{q}$ (see Fano 1963). The first term in square brackets accounts for the 'longitudinal' interaction through the static unretarded Coulomb field; the second term corresponds to the 'transversal' interaction through emission and reabsorption of virtual photons. For the time being, we assume the incident electron as distinguishable from the target electrons and we also neglect any effect related to the spin of the electron. Density effect corrections which lead to a saturation of the ionisation cross section for high incident energies (see e.g. Scofield, 1978) are not included in the present approach. Therefore, our results apply to free atoms rather than to atoms bound in a solid.

Expression (2) contains a purely kinematic factor and the GOS which embodies a complete description of the target concerning inelastic scattering (within the Born approximation). In the limit $Q\to 0$, the GOS reduces to the optical oscillator strength $df(W)/dW$. It is worth recalling that the OOS and the cross section for absorption of a photon with energy W are related by

$$\frac{df(W)}{dW}=\frac{mc}{2\pi^2e^2\hbar}\sigma_{ph}(W) \tag{3}$$

provided the wavelength of the photon is much larger than the 'radius' of the atomic shell where the photoelectric effect takes place (dipole approximation).

The GOS and the complex dielectric function $\varepsilon(Q, W)$ describing the response of any (isotropic) medium to a small electromagnetic disturbance are related by (Fano 1956, Pines 1963)

$$\mathrm{Im}\left[\frac{-1}{\varepsilon(Q,W)}\right]=\frac{\pi\Omega_p^2}{2W}\frac{1}{Z}\frac{df(Q,W)}{dW} \tag{4}$$

where Ω_p is the plasma energy corresponding to the *total* electron density in the material, i.e.

$$\Omega_p^2=4\pi\hbar^2NZe^2/m \tag{5}$$

N being the number of atoms per unit volume.

The GOS is known analytically for only the simplest atomic target, namely the hydrogen atom (see e.g. Inokuti 1971). The complex dielectric function of the free electron gas, derived from the random phase approximation, has been given in closed analytical form by Lindhard (1954). GOSs for atoms and ions have been computed numerically by a number of authors (see references in Powell, 1985) using independent electron models. Besides the large calculation effort to obtain each value of these numerical GOS, additional interpolation and/or extrapolation difficulties arise when computing integrals of the DCS corresponding to different measurable quantities.

The GOS can be represented as a surface over the plane (W, Q) which is known as the Bethe surface (Inokuti 1971). For large values of W, the GOS vanishes except for $Q\simeq W$ and the Bethe surface reduces to a ridge, the Bethe ridge, which peaks around

the line $Q = W$. Indeed, in the high-W limit, binding effects are small and the GOS may be evaluated by assuming the target electrons are free and at rest, this gives

$$\frac{\mathrm{d}f(Q, W)}{\mathrm{d}W} \simeq Z\delta(W - Q). \tag{6}$$

Actually the Bethe ridge has a finite width which arises from the momentum distribution of the atomic electrons. For small recoil energies ($Q \ll W$), we have

$$\frac{\mathrm{d}f(Q, W)}{\mathrm{d}W} \simeq \frac{\mathrm{d}f(W)}{\mathrm{d}W}. \tag{7}$$

In the limited range of Q values where this relation holds, the DCS (2) decreases rapidly with Q. It follows that the key quantity to determine the DCS for low-Q excitations is the OOS. On the other hand, it is known that useful average quantities such as the total inelastic cross section and the stopping cross section for incident electrons of high kinetic energies are completely determined by the OOS distribution (see Inokuti 1971). In particular, the mean excitation energy, which is the most important parameter entering the Bethe stopping power formula, is given by

$$\ln(I) = \frac{1}{Z}\int_0^\infty \ln(W)\frac{\mathrm{d}f(W)}{\mathrm{d}W}\,\mathrm{d}W. \tag{8}$$

3. Statistical models

Once the two asymptotic limits (6) and (7) have been specified, the remaining task in order to construct a schematised Bethe surface model is to specify a suitable interpolation algorithm to generate the GOS for intermediate recoil energies. If the algorithm is physically sound and simple enough, we may expect to obtain an accurate DCS with only a moderate amount of numerical work. Studies along these lines are due to Tung *et al* (1979), Ashley (1982, 1988) and Penn (1987). The statistical models proposed by these authors have been given in the context of the non-relativistic dielectric formalism, we give here an alternative description to them from the atomistic point of view, i.e. using the GOS concept.

The starting point of the statistical models to be described is the OOS. Nowadays, a great deal of experimental information on the OOS distribution is available either in the form of optical data (Palik 1985) or as photoabsorption cross sections (Hubbell 1971, Veigele 1973).

Tung *et al* (1979) adopted the OOS obtained from the local plasma approximation (LPA) of Lindhard and Scharff (1953) by using Dirac-Hartree-Slater atomic electron densities $\rho(\boldsymbol{r})$ computed under Wigner-Seitz boundary conditions. The LPA sets the OOS spectrum as

$$\left[\frac{\mathrm{d}f(W)}{\mathrm{d}W}\right]_{\mathrm{LPA}} = \int_0^\infty \rho(\boldsymbol{r})\delta(W - \chi W_p(\boldsymbol{r}))\,\mathrm{d}\boldsymbol{r} \tag{9}$$

where $W_p(\boldsymbol{r})$ is the local plasmon energy, i.e.

$$W_p^2(\boldsymbol{r}) = 4\pi\hbar^2\rho(\boldsymbol{r})e^2/m \tag{10}$$

and χ is a constant which Tung *et al* set at unity. It may be shown that their approach is equivalent to using the following GOS

$$\left[\frac{\mathrm{d}f(Q, W)}{\mathrm{d}W}\right]_{\text{Tung}} = \int_0^{\infty} \left[\frac{\mathrm{d}f(W')}{\mathrm{d}W'}\right]_{\text{LAP}} F_L(W'; Q, W)\,\mathrm{d}W' \tag{11}$$

where $F_L(W'; Q, W)$ is the GOS per electron corresponding to Lindhard's dielectric function ε_L for an electron gas characterised by the plasmon energy W', thus

$$F_L(W'; Q, W) = \frac{2W}{\pi(W')^2}\,\mathrm{Im}\left(\frac{-1}{\varepsilon_L(W'; Q, W)}\right). \tag{12}$$

It can be seen that the use of F_L guarantees the correct high-Q behaviour of the GOS and, moreover, the resulting Bethe ridge has a finite width reflecting the momentum distribution of the electrons in the target. However we may note that the OOS derived from the LPA is only roughly approximate. In particular, this approximation leads to a value of the mean excitation energy (8) that may differ appreciably from its actual value, i.e. the value obtained from (8) using the experimental OOS. This value can be reproduced by using a suitable value of the parameter χ in (10).

Ashley (1982, 1988) uses a similar model which incorporates experimental OOSS, thus avoiding the major limitation of the previous statistical model, and accounts for exchange effects in an approximate way. At the same time, to facilitate further calculations, he introduced the following one-mode approximation

$$F_A(W'; Q, W) = \delta(W - W_r),\ W_r \equiv W' + Q \tag{13}$$

for the GOS per electron. As pointed out by Ashley (1982), this one-mode approximation gives nearly the same dispersion relation as Lindhard's theory in the low-Q limit as well as leading to the proper high-Q limit, $W \simeq Q$. Thus, Ashley's model is equivalent to the GOS

$$\left[\frac{\mathrm{d}f(Q, W)}{\mathrm{d}W}\right]_{\text{Ashley}} = \int_0^{\infty} \left[\frac{\mathrm{d}f(W')}{\mathrm{d}W'}\right]_{\text{exp}} F_A(W'; Q, W)\,\mathrm{d}W'. \tag{14}$$

Hereafter, $[\mathrm{d}f(W)/\mathrm{d}W]_{\text{exp}}$ stands for the OOS derived from available experimental data.

The statistical model proposed by Penn (1987) combines the advantages of the two previous models: It incorporates experimental OOSS and it uses the Lindhard GOS per electron to generate the GOS for $Q > 0$. Thus, Penn's GOS is given by

$$\left(\frac{\mathrm{d}f(Q, W)}{\mathrm{d}W}\right)_{\text{Penn}} = \int_0^{\infty} \left(\frac{\mathrm{d}f(W')}{\mathrm{d}W'}\right)_{\text{exp}} F_L(W'; Q, W)\,\mathrm{d}W'. \tag{15}$$

These non-relativistic models have mainly been used to compute inelastic mean free paths of low energy electrons in condensed matter; Ashley (1988) also gives stopping powers. For comparison of the results from the different models the reader is referred to the original papers. We merely indicate that mean free paths from Ashley's and Penn's models agree to within 5% for electron energies between 100 eV and 10 keV (Ashley 1988).

In what follows we consider the evaluation of the DCS for K-shell ionisation of neutral atoms. As mentioned before, the experimental OOS (i.e. the photoelectric cross section) is accurately reproduced by a simple hydrogenic model. Following Egerton (1986), we introduce the screening effects through an effective nuclear charge $Z_s = Z - 0.3$, incorporating the screening of the second $1s$ electron, and a binding energy

reduction E_s which accounts for the screening of the outer electron shells. This last quantity is obtained from the observed ionisation threshold energy U_K as $E_s = U_H - U_K$ where $U_H = Z_s^2 me^4/(2\hbar^2)$. The hydrogenic OOS for K-shell ionisation is given in terms of the dimensionless variable $\kappa^2 = W/U_H - 1$ by

$$\frac{df_K(W)}{dW} = \frac{256U_H^3}{3W^4}\frac{\exp\{-(2/\kappa)\tan^{-1}(2\kappa/[1-\kappa^2])\}}{1-\exp(2\pi/\kappa)} \qquad \text{if } \kappa^2 > 0$$

$$= \frac{256U_H^3}{3W^4}\exp\left[-(-\kappa^2)^{-1/2}\ln\left(\frac{1-\kappa^2+2(-\kappa^2)^{1/2}}{1-\kappa^2-2(-\kappa^2)^{1/2}}\right)\right] \qquad \text{if } \kappa^2 < 0. \tag{16}$$

(When $Z = 1, 2$, we take $U_H = U_K$ and $E_s = 0$.) This OOS has a characteristic saw-tooth profile which starts at the ionisation threshold $W = U_K$ and decreases monotonically as the energy loss increases. Hereafter, we consider (16) as the 'experimental' OOS associated with K-shell ionisation.

The statistical models described above lead to realistic results for low energy electrons, i.e. when the majority of excitations correspond to the outer shells or to the conduction band. However, they are not suitable for describing inner-shell ionisation. To clarify this feature, let us consider the case of K-shell ionisation. The model of Penn generates a GOS which does not vanish for energy losses less than the ionisation threshold U_K and, therefore, it gives a finite cross section for excitations with $W < U_K$. On the other hand, Ashley's model shifts the ionisation threshold to $2U_K$, i.e. only electrons with kinetic energy larger than $2U_K$ can produce ionisations. This is so because the region of kinematically allowed excitations in the (Q, W) plane does not overlap the region $W > U_K + Q$ where Ashley's GOS is nonvanishing unless $E > 2U_K$.

In the present work we consider a new statistical model that is more suited for describing inner-shell ionisation. In a less elaborate form, this model was used by Liljequist (1983, 1985) and by Salvat *et al* (1985) to provide simple estimates of the inelastic cross sections suited for Monte Carlo simulation of electron transport. For practical reasons, the OOSS adopted by these authors were only roughly approximate; they were extrapolated for $Q > 0$ by using the function

$$F_\delta(W'; Q, W) = \delta(W - W')\theta(W' - Q) + \delta(W - Q)\theta(Q - W'). \tag{17}$$

In our statistical model we introduce experimental OOSS (or expression (16) in the case of K-shell ionisation) and we use the simple function (17) as the GOS per electron. The resulting GOS is

$$\left[\frac{df(Q, W)}{dW}\right]_L = \int_0^\infty \left[\frac{df(W')}{dW'}\right]_{exp} F_\delta(W'; Q, W)\, dW' \tag{18}$$

which may be written in the more explicit form

$$\left[\frac{df(Q, W)}{dW}\right]_L = \left[\frac{df(W)}{dW}\right]_{exp} \theta(W - Q) + h(Q)\delta(W - Q) \tag{19}$$

with

$$h(Q) = \int_0^Q \left[\frac{df(W)}{dW}\right]_{exp} dW = Z - \int_Q^\infty \left[\frac{df(W)}{dW}\right]_{exp} dW \tag{20}$$

where the last equality follows from the Bethe sum rule. The corresponding Bethe surface vanishes for $Q > W$, in the region $Q < W$ it is modulated by the OOS along the direction of the W axis and it is constant along the Q axis direction. The Bethe ridge

originates from the second term in (17), it reduces to the delta function $\delta(W-Q)$ weighted by the function $h(Q)$. Thus, the model clearly separates the distant ($Q<W$) collisions and the close ($Q=W$) collisions. It is clear that the statistical model (19, 20) leads to the correct threshold for bound shell ionisation. Indeed, it reproduces reasonably well the dependence on Q of the GOS for energy losses near the ionisation threshold (see Inokuti 1971). The unrealistic zero width of the Bethe ridge means that, in close collisions, the target electrons behave as though they were *free and at rest.*

4. Exchange and low energy corrections

Important quantities, such as the total cross section and the stopping cross section, are obtained from the energy loss DCS, which is defined by

$$\frac{\mathrm{d}\sigma}{\mathrm{d}W}=\int\frac{\mathrm{d}^2\sigma}{\mathrm{d}Q\,\mathrm{d}W}\mathrm{d}Q \tag{21}$$

where the integral extends over the interval of kinematically allowed recoil energies. Let us now evaluate the energy loss DCS from the GOS given by (19). We begin by considering the contribution due to close collisions, i.e. to excitations in the Bethe ridge. As stated above, the target electrons behave as though they were free and at rest; the effect of binding is included through the $h(Q)$ function, which gives the effective number of target electrons that participate in collisions involving an energy loss $W=Q$. The relativistic Born DCS for binary collisions with free electrons at rest is given by the Moller formula

$$\frac{\mathrm{d}\sigma_{\mathrm{M}}(E,W)}{\mathrm{d}W}=\frac{2\pi e^4}{mv^2}\left[\frac{1}{W^2}+\frac{1}{(E-W)^2}-\frac{1}{W(E-W)}+\left(\frac{\gamma-1}{\gamma}\right)^2\left(\frac{1}{E^2}+\frac{1}{W(E-W)}\right)\right] \tag{22}$$

which incorporates exchange effects. Here $\gamma=1+E/mc^2$ and the maximum energy loss is $W_{\max}=E/2$. Thus, the energy loss DCS for close collisions with the statistical model (19) is obtained as

$$\frac{\mathrm{d}\sigma_{\mathrm{c}}}{\mathrm{d}W}=h(W)\frac{\mathrm{d}\sigma_{\mathrm{M}}(E,W)}{\mathrm{d}W}. \tag{23}$$

The relativistic energy loss DCS for distant collisions ($Q<W$) takes the following analytical expression

$$\frac{\mathrm{d}\sigma_{\mathrm{d}}}{\mathrm{d}W}\equiv\frac{2\pi e^4}{mv^2}\frac{1}{W}\left(\frac{\mathrm{d}f(W)}{\mathrm{d}W}\right)_{\mathrm{exp}}\left[\ln\left(\frac{W(Q_-+2mc^2)}{Q_-(W+2mc^2)}\right)+\ln\left(\frac{1}{1-\beta^2}\right)-\beta^2\right] \tag{24}$$

where Q_- is the minimum recoil energy

$$Q_-=[\{[E(E+2mc^2)]^{1/2}\pm[(E-W)(E-W+2mc^2)]^{1/2}\}^2+m^2c^4]^{1/2}-mc^2. \tag{25}$$

The energy loss DCS is thus given by

$$\frac{\mathrm{d}\sigma}{\mathrm{d}W}=\frac{\mathrm{d}\sigma_{\mathrm{c}}}{\mathrm{d}W}+\frac{\mathrm{d}\sigma_{\mathrm{d}}}{\mathrm{d}W}. \tag{26}$$

It is well known that the Born approximation overestimates the cross sections for relatively small kinetic energies of the incident electron. This is mainly due to the distortion of the incident electron wavefunction due to the electrostatic field of the

target. This field produces an increase in the effective kinetic energy of the incident electron and is expected to be important in close collisions. Although it is very difficult to introduce this effect accurately, we may proceed in analogy with the classical theory of binary collisions (see Salvat *et al* 1985) and assume that the incident electron gains a kinetic energy $2U_K$ before it interacts with a target electron, which is bound with binding energy U_K. The maximum energy loss is taken to be $W_{max}=(E+U_K)/2$, i.e. the allowed energy losses lie in the interval $U_K < W < W_{max}=(E+U_K)/2$. With this correction, the ionisation cross section near the threshold is reduced, thus yielding better agreement with experimental data (see below).

5. The Weizsacker–Williams method of virtual quanta

This method (Jackson 1975) exploits the fact that the electromagnetic field produced by a fast charged particle at the position of a point target is equivalent to the superposition of two pulses of plane polarised radiation impinging on the target in directions parallel and perpendicular to the momentum $\boldsymbol{p}$ of the incident particle. This method has been applied to the evaluation of inner-shell ionisation cross sections by electron impact by Kolbenstvedt (1967) and by Seltzer and Berger (1982).

Let us consider an electron with kinetic energy E passing a target atom with impact parameter b. Fourier analysis of the perturbing field of the moving particle yields the following frequency spectrum (energy per unit area and unit frequency interval measured at the target position)

$$\frac{\mathrm{d}I(\omega,b)}{\mathrm{d}\omega}=\frac{e^2}{\pi^2 c}\frac{1}{\beta^2 b^2}\left(\frac{\omega b}{\gamma v}\right)^2\left[K_1^2\left(\frac{\omega b}{\gamma v}\right)+\gamma^{-2}K_0^2\left(\frac{\omega b}{\gamma v}\right)\right] \tag{27}$$

where K_0 and K_1 are modified Bessel functions. The flux of virtual quanta, $\mathrm{d}N(W,b)$ ($W=\hbar\omega$) is obtained by using the relation

$$\begin{aligned}\frac{\mathrm{d}N(W,b)}{\mathrm{d}W}\mathrm{d}W&=\frac{1}{\hbar\omega}\frac{\mathrm{d}I(\omega,b)}{\mathrm{d}\omega}\mathrm{d}\omega\\&=\frac{e^2}{\pi^2\hbar c}\frac{1}{\beta^2 b^2}\left(\frac{Wb}{\gamma v}\right)^2\left[K_1^2\left(\frac{Wb}{\gamma v}\right)+\gamma^{-2}K_0^2\left(\frac{Wb}{\gamma v}\right)\right]\frac{1}{W}\mathrm{d}W.\end{aligned} \tag{28}$$

Each of these virtual photons with energy larger than the ionisation threshold can now ionise the atom by the photoelectric effect. The ionisation DCS associated with impact parameters larger than b_{min} is then

$$\frac{\mathrm{d}\sigma}{\mathrm{d}W}(b>b_{min})=\sigma_{ph}(W)\frac{\mathrm{d}N(W)}{\mathrm{d}W} \tag{29}$$

where

$$\begin{aligned}\frac{\mathrm{d}N(W)}{\mathrm{d}W}&=\int_{b_{min}}^{\infty}\frac{\mathrm{d}N(W,b)}{\mathrm{d}W}2\pi b\,\mathrm{d}b\\&=\frac{e^2}{\pi\hbar c\beta^2}\frac{1}{W}\{2xK_0(x)K_1(x)-\beta^2x^2[K_1^2(x)-K_0^2(x)]\}\end{aligned} \tag{30}$$

with

$$x\equiv\frac{Wb_{min}}{\hbar\gamma v}. \tag{31}$$

Using (3) the DCS given by (28) can be finally written as

$$\frac{d\sigma}{dW}(b > b_{min}) = \frac{2\pi e^4}{mv^2}\frac{1}{W}\left[\frac{df(W)}{dW}\right]_{exp}\{2xK_0(x)K_1(x) - \beta^2 x^2[K_1^2(x) - K_0^2(x)]\}. \quad (32)$$

For low energy losses ($x \ll 1$) it reduces to

$$\frac{d\sigma}{dW}(b > b_{min}) \simeq \frac{2\pi e^4}{mv^2}\frac{1}{W}\left[\frac{df(W)}{dW}\right]_{exp}\left\{2\ln\left(\frac{1.123}{x}\right) - \beta^2\right\}. \quad (33)$$

This procedure only gives the DCS for distant collisions. Close collisions, corresponding here to impact parameters smaller than b_{min}, may be described as binary collisions with free electrons at rest, i.e. through the Moller DCS (22)

$$\frac{d\sigma}{dW}(b < b_{min}) = Z_K \frac{d\sigma_M(E, W)}{dW} \quad (34)$$

where Z_K is the number of electrons in the considered shell.

The minimum impact parameter b_{min} is usually taken as the Bohr radius of the shell (see Kolbenstvedt 1967). We note that expressions (24) and (33) coincide when the arguments of the logarithms are the same. This leads to the following estimate of the minimum impact parameter

$$b_{min} = 1.123\hbar/(2mW)^{1/2}. \quad (35)$$

Assuming there is a correspondence between recoil energy and impact parameter (i.e. large impact parameters correspond to small recoil energies and *vice versa*) and that the Born approximation holds, we are forced to replace W in (35) by the *minimal* energy loss U_K since otherwise the DCS for distant collisions will contain contributions from excitations already accounted for in the DCS for close collisions—note that (34) contains Z_K rather than the fraction $h(W)$ appearing in (23). We therefore set

$$b_{min} = 1.123\hbar/(2mU_K)^{1/2}. \quad (36)$$

It is interesting to observe that for the K-shell hydrogenic model without screening $U_K = Z^2me^4/(2\hbar^2)$ and the Bohr radius is $a = \hbar^2/Zme^2$; in this case we have

$$b_{min} = 1.123\hbar/(2mU_K)^{1/2} = 1.123a \quad (37)$$

in good agreement with the usual estimate $b_{min} = a$.

Improvement of the computed cross section near the threshold is obtained by introducing the empirical low energy correction described in the previous section. It may already be anticipated that the cross sections obtained from our statistical model—equations (23) and (24)—and from the method of virtual quanta—equations (32) and (34)—will be practically equivalent—except near the threshold due to the effect of the $h(W)$ function in equation (21). Actually, the Weizsacker-Williams method, using equation (33) instead of (32) and the value of the minimum impact parameter given by (36), is *exactly* equivalent to the statistical model derived from the following GOS per electron:

$$F_{WW}(W'; Q, W) \equiv \delta(W - W')\theta(U_K - Q) + \delta(W - Q)\theta(Q - U_K) \quad (38)$$

which does not differ very much from (17). We may then conclude that the simple

expression (17) of the GOS per electron for $Q < W$ incorporates physical assumptions similar to those involved in equation (29).

6. Comparison with experimental data

The numerical evaluation of the ionisation cross section

$$\sigma_K \equiv \int \frac{d\sigma}{dW} dW \tag{39}$$

now requires only a single quadrature.

The ionisation cross section of hydrogen is shown in figure 1 as a function of the kinetic energy of the incident electron. It is seen that our statistical model and the Weizsacker-Williams method are in close agreement for energies above the maximum of the cross section and give a good average description of the experimental data in this energy range. The non-relativistic Born cross section, derived from the GOS of the hydrogen atom, is also included for comparison; this cross section does not differ very much from that obtained with our GOS model *without* the low energy correction. The improvement due to this correction is seen to be noticeable for energies near the ionisation threshold.

Ionisation cross sections for helium are plotted in figure 2. Again, the agreement with experimental data is quite good for energies above the maximum of the cross section. As for hydrogen, our theoretical calculations shift this maximum to lower energies. A similar shift is obtained with the Born approximation (Rudge 1968).

In practice (see e.g. Kolbenstvedt 1967), Weizsacker-Williams calculations are performed by using approximation (33) instead of the rigorous result (32). This

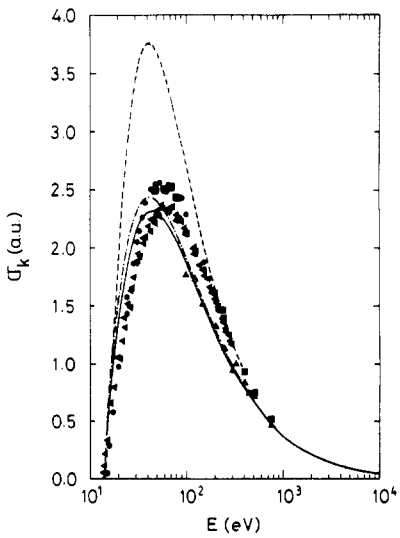

Figure 1. Ionisation cross sections for hydrogen in atomic units. The continuous and chain curves are the cross sections obtained from our statistical model and from the Weizsacker-Williams method respectively (with low energy correction included). The broken curve is the result of the Born approximation (Rudge 1968). Experimental data are those reported by Kieffer and Dunn (1966).

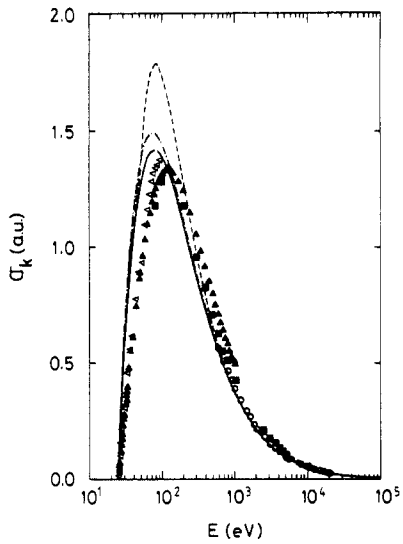

Figure 2. Ionisation cross sections for helium. The broken curve has been obtained from our statistical model without low energy correction. Other details are the same as in figure 1.

replacement slightly changes the ionisation cross section as shown in figure 3. The effect of the low energy correction on the Weizsacker-Williams cross section is also indicated. The uncorrected Weizsacker-Williams cross section shows a slight elbow at $W = 2U_K$ due to the sudden start of the close collision contribution.

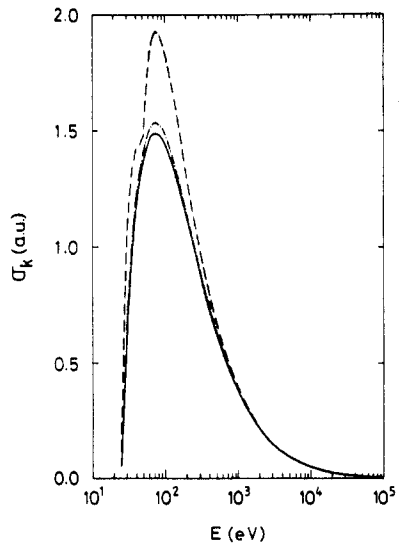

Figure 3. Ionisation cross sections for helium as given by the Weizsacker-Williams method. The full and broken curves are the cross sections derived from (32) with and without low energy correction respectively. The chain curve gives the ionisation cross section computed from the approximate DCS (33).

Results for aluminium and nickel are shown in figure 4; again the agreement between the theoretical and experimental data is fairly good, even near the thresholds. It is interesting to note that the ionisation cross section takes a minimum value near 1 MeV and it increases monotonically for increasing energies as a consequence of relativistic effects. The *ab initio* calculation of Scofield (1978) for nickel is also shown. Figure 5 contains the K-shell ionisation cross section for gold. In this case agreement is not so clear because of the scattered experimental data. For high atomic numbers the use of the (non-relativistic) hydrogenic model is questionable since relativistic effects on the target electron wavefunction are known to be important; this deficiency could be partially amended by using experimental photoionisation data.

K-shell ionisation cross sections for 100 keV electrons and a number of elements through the periodic system have been measured by Westbrook and Quarles (1987). Their results are given in figure 6, which also includes our calculations and the

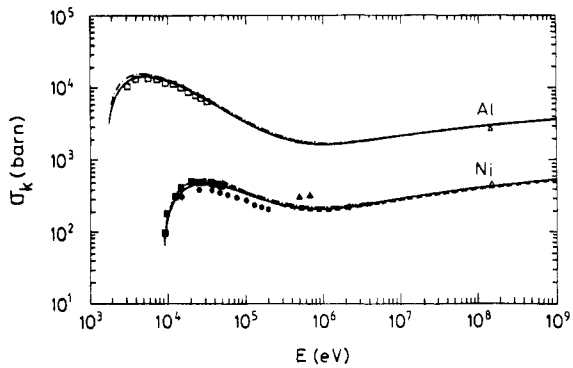

Figure 4. K-shell ionisation cross sections for aluminium and nickel. The full and chain curves give the results from our approximate GOS and from the Weizsacker-Williams method respectively (including low energy correction). The broken curve is the theoretical Born cross section computed by Scofield (1978) for Ni. Experimental data are from: Ishii *et al* (1977), △; Hink and Ziegler (1969), □; Li-Scholtz *et al* (1973), ◀; Seif el Nasr *et al* (1974), ▲; Pockman *et al* (1947), ●; Jessenberger and Hink (1975), ■.

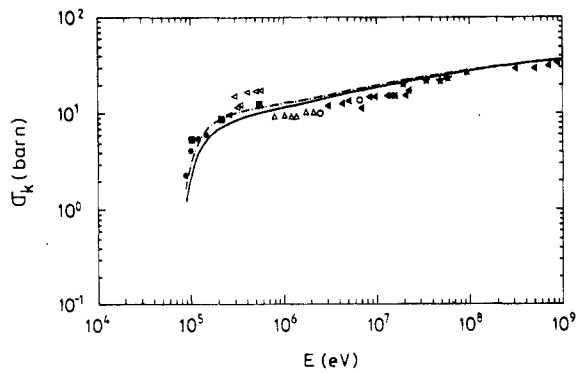

Figure 5. K-shell ionisation cross section for gold. Details are the same as in figure 4. Experimental data are from: Davis *et al* (1972), ●; Motz and Placious (1964), ■; Hansen and Flammersfeld (1966), ◁; Rester and Dance (1966), △; Dangerfield and Spicer (1975), ◀; Berkner *et al* (1970), ○; Hoffman *et al* (1978), ★; Ishii *et al* (1977), ▲.

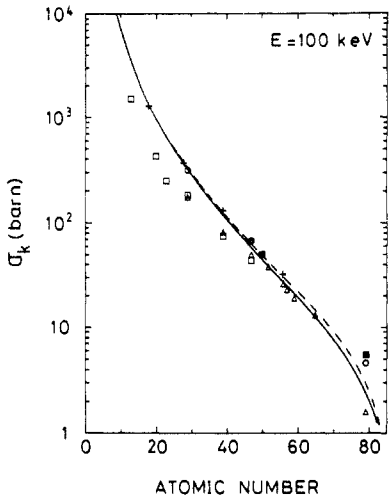

Figure 6. K-shell ionisation cross section for 100 keV electrons as a function of the atomic number. The full and broken curves give the results from our approximate GOS and from the Weizsacker-Williams method respectively (including low energy correction). Experimental data are from: Westbrook and Quarles (1987), △ and □; Davis *et al* (1972), ○; Motz and Placious (1964), ■. The results of the *ab initio* Born calculations of Scofield (1978) are also shown (+).

theoretical results of Scofield (1978). On the whole, the agreement between our results and the experimental data is again satisfactory. For low atomic numbers, i.e. when the kinetic energy E is much larger than the ionisation threshold, our results practically coincide with those of Scofield. The slight differences for higher Z arise mainly from the low energy correction introduced in our model.

7. Conclusions

The results of the last section confirm the validity of the present statistical model for energies in the range from the K-shell ionisation threshold up to highly relativistic energies. With the introduction of the low-energy correction, a substantial improvement of the computed cross sections near the ionisation threshold has been obtained. For ionisations of other shells we may expect to obtain results of similar quality provided the proper photoelectric cross section or (experimental) OOS is used.

The analysis in section 5 evidences the close relationship between the present statistical model and the Weizsacker-Williams method of virtual quanta. The equivalence between both approaches enlightens the physical assumptions underlying our model which may now be considered as an alternative formulation of the method of virtual quanta.

Acknowledgments

We are deeply indebted to D Liljequist for his interest and valuable suggestions on the present work.

References

Ashley J C 1982 *J. Electron Spectrosc. Relat. Phenom.* **28** 177
—— 1988 *J. Electron Spectrosc. Relat. Phenom.* **46** 199
Berkner K H, Kaplan S N and Pyle R V 1970 *Bull. Am. Phys. Soc.* **15** 786
Dangerfield G R and Spiecer B M 1975 *J. Phys. B: At. Mol. Phys.* **8** 1744
Davies D V, Mistry V D and Quarles C A 1972 *Phys. Lett.* **35A** 169
Egerton R F 1986 *Electron Energy Loss Spectroscopy in the Electron Microscope* (New York: Plenum)
Fano U 1956 *Phys. Rev.* **103** 1202
—— 1963 *Ann. Rev. Nucl. Sci.* **13** 1
Fano U and Cooper J W 1968 *Rev. Mod. Phys.* **40** 441
Hansen H and Flammersfeld A 1966 *Nucl. Phys.* **79** 135
Hink W and Ziegler A 1969 *Z. Phys.* **226** 222
Hoffman H H, Genz H, Löw W and Richter A 1978 *Phys. Lett.* **65A** 304
Hubbell J H 1971 *At. Data Tables* **3** 241
Inokuti M 1971 *Rev. Mod. Phys.* **43** 297
Ishii K, Kamiya M, Sera K, Morita S, Tawara H, Oyamada M and Chu T C 1977 *Phys. Rev.* A **15** 906
Jackson J D 1975 *Classical Electrodynamics* (New York: Wiley)
Jessenberger J and Hink W 1975 *Z. Phys.* A **275** 331
Kieffer G and Dunn G H 1966 *Rev. Mod. Phys.* **38** 1
Kolbenstvedt H 1967 *J. Appl. Phys.* **18** 4785
Li-Scholz A, Collé R, Preiss I L and Scholz W 1973 *Phys. Rev.* A **7** 1957
Liljequist D 1983 *J. Phys D: Appl. Phys.* **16** 1567
—— 1985 *J. Appl. Phys.* **57** 657
Lindhard J 1954 *Danske Mat. Fys. Meddr.* **28** n8 1
Lindhard J and Scharff M 1953 *Danske Mat. Fys. Meddr.* **27** n15 1
Mayol R and Salvat F 1989 *Internal report* University of Barcelona (unpublished)
Motz J W and Placious R C 1964 *Phys. Rev.* **136** A662
Palik E D 1985 (ed) *Handbook of Optical Constants of Solids* (Academic, New York)
Penn D R 1987 *Phys. Rev.* B **35** 482
Pines D 1963 *Elementary Excitations of Solids* (Benjamin, New York)
Pockman L T, Webster D L, Kirkpatrick P and Harworth K 1947 *Phys. Rev.* **71** 330
Powell C J 1985 in *Electron Impact Ionization* ed T D Mark and G H Dunn (Wien: Springer)
Rester D H and Dance W E 1966 *Phys. Rev.* **152** 1
Rudge M R H 1968 *Rev. Mod. Phys.* **40** 564
Salvat F, Martínez J D, Mayol R and Parellada J 1985 *J. Phys. D: Appl. Phys.* **18** 299
Scofield J H 1978 *Phys. Rev.* A **18** 963
Seif el Nasr S A H, Berényi D and Bibok Gy 1974 *Z. Phys.* **267** 169
Seltzer S M and Berger M J 1982 *National Bureau of Standards Report* NBSIR 82-2572
Tung C J, Ashley J C and Ritchie R H 1979 *Surf. Sci.* **81** 427
Veigele W J 1973 *At. Data Tables* **5** 51
Westbrook G L and Quarles C A 1987 *Nucl. Instrum. Methods* B **24/25** 196